INTERIM REPORT

High Sensitivity Magnetoresisitive Sensors for both DC and EMI Magnetic Field Mapping

SERDP Project MR-1716

MAY 2012

Sy-Hwang Liou
University of Nebraska

SERDP
DOD ▪ EPA ▪ DOE

Report Documentation Page

Form Approved
OMB No. 0704-0188

1. REPORT DATE	2. REPORT TYPE	3. DATES COVERED
MAY 2012	**N/A**	**-**

4. TITLE AND SUBTITLE	5a. CONTRACT NUMBER
High Sensitivity Magnetoresisitive Sensors for both DC and EMI Magnetic Field Mapping	5b. GRANT NUMBER
	5c. PROGRAM ELEMENT NUMBER
6. AUTHOR(S)	5d. PROJECT NUMBER
	5e. TASK NUMBER
	5f. WORK UNIT NUMBER
7. PERFORMING ORGANIZATION NAME(S) AND ADDRESS(ES) **University of Nebraska**	8. PERFORMING ORGANIZATION REPORT NUMBER
9. SPONSORING/MONITORING AGENCY NAME(S) AND ADDRESS(ES)	10. SPONSOR/MONITOR'S ACRONYM(S)
	11. SPONSOR/MONITOR'S REPORT NUMBER(S)

12. DISTRIBUTION/AVAILABILITY STATEMENT
Approved for public release, distribution unlimited

13. SUPPLEMENTARY NOTES
The original document contains color images.

14. ABSTRACT

15. SUBJECT TERMS

16. SECURITY CLASSIFICATION OF:			17. LIMITATION OF ABSTRACT	18. NUMBER OF PAGES	19a. NAME OF RESPONSIBLE PERSON
a. REPORT	b. ABSTRACT	c. THIS PAGE			
unclassified	**unclassified**	**unclassified**	**SAR**	**18**	

Standard Form 298 (Rev. 8-98)
Prescribed by ANSI Std Z39-18

This report was prepared under contract to the Department of Defense Strategic Environmental Research and Development Program (SERDP). The publication of this report does not indicate endorsement by the Department of Defense, nor should the contents be construed as reflecting the official policy or position of the Department of Defense. Reference herein to any specific commercial product, process, or service by trade name, trademark, manufacturer, or otherwise, does not necessarily constitute or imply its endorsement, recommendation, or favoring by the Department of Defense.

Table of Contents

Acronyms:

AFM – Antiferromagnetic
DAQ – data acquisition
DMM - discarded military munitions
EMI – electromagnetic induction
FM – ferromagnetic
HPF - high-pass-filter
LPF - low-pass-filter
MEC- munitions and explosives of concern
MTJ - magnetic tunnel junction
MFC - magnetic flux concentrators

MFC - magnetic flux concentrators
MR – magnetoresistance
RA - resistance time area

pT - the picotesla (10^{-12} tesla)
QFS - Quasar Federal Systems, Inc
TMR – Tunneling magnetoresistance
UXO – unexploded ordnance
ΔR - the change in resistance

High Sensitivity Magnetoresisitive Sensors for both DC and EMI Magnetic Field Mapping

SERDP Project MM-1716
Principal Investigator: Sy-Hwang Liou and Yongming Zhang

1. BACKGROUND

The current magnetic sensors that are used to detect unexploded ordnance (UXO) and discarded military munitions (DMM) are bulky and require relatively large spacing (0.25 to 0.5 m). Some of these sensor systems are capable of dual-mode operation; however, they are only of limited frequency range (typical <20 kHz). Develop advanced magnetics sensor array is important for classification of smaller (less than 37 mm projectiles), deep targets or multiple targets etc.

2. OBJECTIVE

The objective of this project is to investigate a lightweight, low-power, compact, practical high-sensitivity magnetic sensor system suitable for both DC and wide frequency band electromagnetic induction (EMI) magnetic field mapping, based on solid-state magnetic tunneling junction (MTJ) devices with a sensitivity in a few tenth picotesla (~ 10^{-12} tesla) range.

The goal of the proposed MTJ sensor are as follows:

- 3-axis vector capability
- Detection of UXO targets to the depth of interest (1-2 meter)
- Measurements can characterize target shape
- Reduction of false alarm rate

BENEFIT: In this project, MTJ sensors will be developed for the purpose of EMI and magnetic signal detection. High bandwidth, low power, light weight, high sensitivity and low cost will provide enhancements to the probability of detection and discrimination of small UXO items and for applications in difficult geology, terrain, and complex ordnance and clutter distributions. The magnetic sensor can also be used in other applications such as vehicle surveillance and orientation control. (Anticipated Project Completion - 2014)

Fig.1 high density three dimensional magnetic sensor array

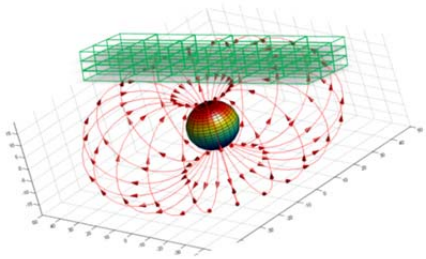

3. TECHNICAL APPROCH:

Challenge I: The goal is to achieve a sensitivity of a few tenth pT/Hz$^{1/2}$ at 1 Hz. We will need to improve sensitivity, reduce noise, in MR sensor

Solutions I:

- MTJ with high TMR ratio (>250%) will possibly improve sensitivity of the MR sensor by a factor of 2 – 3.
- The magnetization of the free layer in MTJ sensor will be easier to rotate using an ultra-soft magnetic layer that will possibly improve the sensitivity of the MR sensor by a factor of 10 – 50
- A better design of magnetic concentrators will possibly improve the sensitivity of the MR sensor by a factor of 10 -1000

Challenge II: Goal is for the sensor response to a field of 0.1 mT to decay to ~100 pT within about 100 μs. This requires 6 decades of linear decay. The issue is that the primary pulse field induces eddy current in the magnetic flux concentrators (MFC) producing a signal in the MFC material that could obscure the early time target signal of the MR sensor.

Solutions II: Select a core material with faster decay Combine with an anti-pulsing approach Subtract digitally if reproducible.

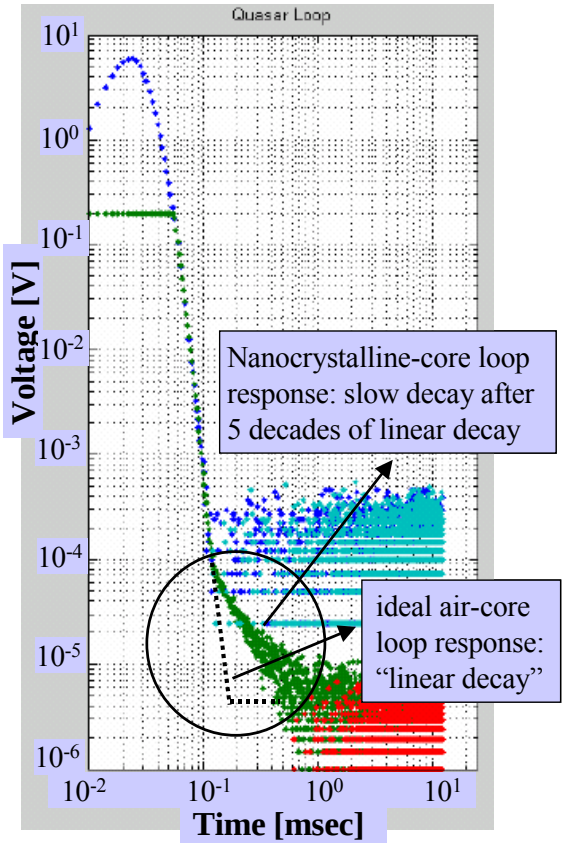

Fig. 2 An example of nanocrystalline-core loop (3" long) and air-coil. The transmit loop is 16 turns, 7 amps, 1m x 1m. The responses in the plot are for sensors at the 16 inches from the side of the coil. In the plots, positive and negative signals are shown with different colors. Curves from two separate tests, one with 10V measurement range (blue for positive, light blue for negative) and one with 0.2V measurement range (green for positive, red for negative), are overlaid to effectively increase the dynamic range of the 12-bit ADC that was used. The transmitter was turned off at 100 μs.

Task 1: Develop high sensitive magnetoresistive sensors (Year 1)

In this task, we have developed a MgO based magnetic tunnel junction with a MR ratio as high as 250% for high sensitive magnetoresistive sensors. The sensor has a sensitivity as high as 4703%/mT. The magnetic sensor only dissipates 1 mW of power while operating under an applied voltage of 1 V. Detail procedures for develop high sensitive MgO-based magnetic tunnel junction (MTJ) sensors is described in Task 1a.

We have also design of a new low noise amplifier for the MTJ sensor that is described in Task 1b. The bandwidth of the amplifier is from DC to 50 kHz.

Task 1a: Develop MgO-based magnetic tunnel junction (MTJ) sensors

We show a few important procedures that improve the sensitivity of our sensors.

- The fabrication of magnetoresistive sensor
- Reducing the magnetic hysteresis by using a coupled soft magnetic layer
- Annealing procedures
- Improving sensitivity of MR sensors using Magnetic Flux Concentrator (MFC)

The Fabrication of magnetoresistive sensor

The typical MTJ layer structure is 1.5 nm Ta/25 nm Ru /7 nm $Ir_{20}Mn_{80}$/2.2 nm $Co_{40}Fe_{60}$/0.85 nm Ru/2.8 nm $Co_{20}Fe_{60}B_{20}$/2 nm MgO/1.5 nm $Co_{20}Fe_{60}B_{20}$/1 nm Ta/15 nm Ru. A Magnetic Tunnel Junction (MTJ) layer design is shown in Fig. 3. The junctions were patterned into ellipses with a size of 10 μm x 15 μm (area 117.8 μm^2, eccentricity 0.74) and a circle with a diameter of 30 μm (area 706.9 μm^2) by photolithography and argon milling. The resistance area product (RA) of MR sensors is typically 10^5 Ω μm^2.

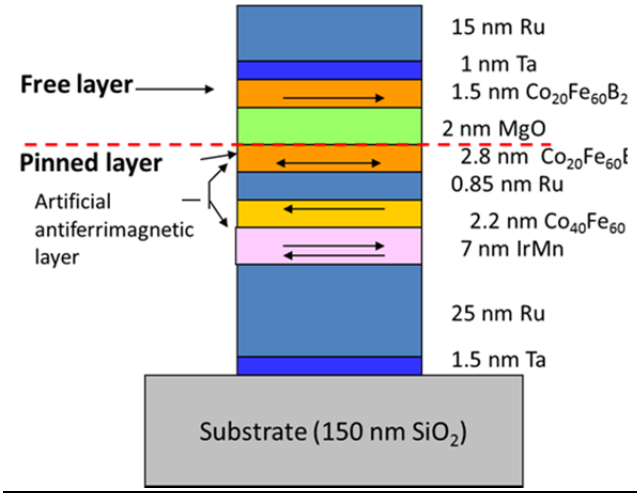

Fig. 3. Magnetic Tunnel Junction (MTJ) layer design

It has been reported early that the magnetic sensor noise will increase the SNR by $N^{1/2}$, where N is the number of MTJ elements either in series or parallel. So, we have designed our magnetic sensor with a 64-element bridge for reducing the noise. The design of the magnetic sensor with a 64-element bridge is shown as follows.

Reducing the magnetic hysteresis by using a coupled soft magnetic layer

The MTJ layer structure for the ferromagnetic–ferro- magnetic coupling study (MTJ-A) is 1.5 nm Ta/15 nm Ru/3 nm $Co_{40}Fe_{60}$/10 nm $Ir_{20}Mn_{80}$/2.2 nm $Co_{40}Fe_{60}$/0.85 nm Ru/2.8 nm $Co_{20}Fe_{60}B_{20}$/2 nm MgO/4 nm $Co_{20}Fe_{60}B_{20}$/10 nm Ta/7 nm Ru. The junctions were patterned into ellipses with a size of 10 μm x 15 μm (area 117.8 μm^2, eccentricity 0.74) by photolithography and argon milling. The MTJ sensor bridge was annealed at 350 ^oC under a 1 T magnetic field for 30 min and a vacuum of 10^{-5} Pa. The pinning direction of the reference layer is along the short axis of the ellipse. By using a coupled soft magnetic layer, we are able to reduce the magnetic hysteresis loss in the free layer and the MTJ junctions could have a better reversibility and linearity around zeromagnetic field, as well as smaller coercivity. We prepare two different free-layer structures from the MTJ-A wafer. First, we remove the 7 nm Ru/10 nm Ta layers by argon milling on the half of the wafer and then deposited 3.3 nm $Ni_{80}Fe_{20}$ /10 nm Ta/7 nm Ru on it. So, all the MTJ junctions are made from the same wafer (i.e., MTJ-A wafer). The MR loops with or without additional $Ni_{80}Fe_{20}$ as a free layer is shown in Fig. 5. The tunneling magneto resistance (TMR) drops from 132% to 115%, which may be due to the reduction of the thickness of $Co_{20}Fe_{60}B_{20}$ free layer during the milling process. The magnetic hysteresis loss in the free layer is reduced by about 42% of the coercivity that is from 4.26 to 2.46 mT. However, the MTJ-A wafer (both samples with or without $Ni_{80}Fe_{20}$) has a large exchange bias, which is not desired for sensor applications. We would prefer to design a magnetic sensor without using an external magnetic bias.

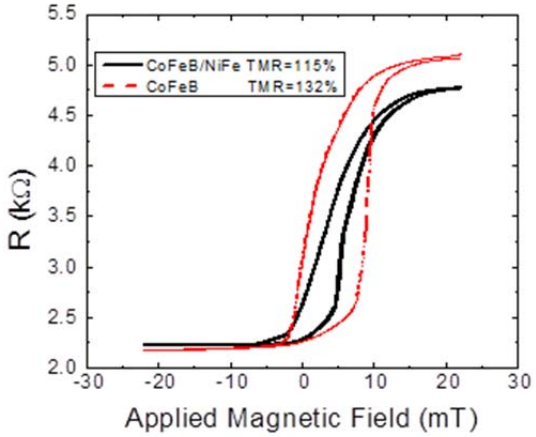

Fig. 5 MR loops of the MTJ-A with the junction area of 10 μm x 15 μm, which have the same pinned layer structure. (a) Dashed line represents that the MTJ-A has 4 nm $Co_{20}Fe_{60}B_{20}$ as a free layer. (b) Solid line represents that the MTJ-A has 4 nm $Co_{20}Fe_{60}B_{20}$ and additional 3.3 nm $Ni_{80}Fe_{20}$ as a free layer

Annealing procedures

The tunneling magnetetoresistance of 250%, and coercivity of about 1 mT was obtained by a multiple-steps annealing procedure. According to our previously work, we get the conclusion that annealing at a lower temperature and under a high magnetic field along short axis of the ellipse (setting the pin layer direction) will help to form a better crystal orientation and decrease defects in the Pin layer of the MR sensor. The sample was usually annealed at 300^oC under 1T magnetic field in the direction along the short axis of the ellipse (setting the pin layer direction), and then annealed 350^oC under 0.1 T along the long axis of the ellipse. The second annealing process helps the magnetization in free layer that keeps as the magnetic dipole, which could rotate smoothly with decreasing the magnetic field. After the annealing, the RH loop was represented as the Fig. 6.

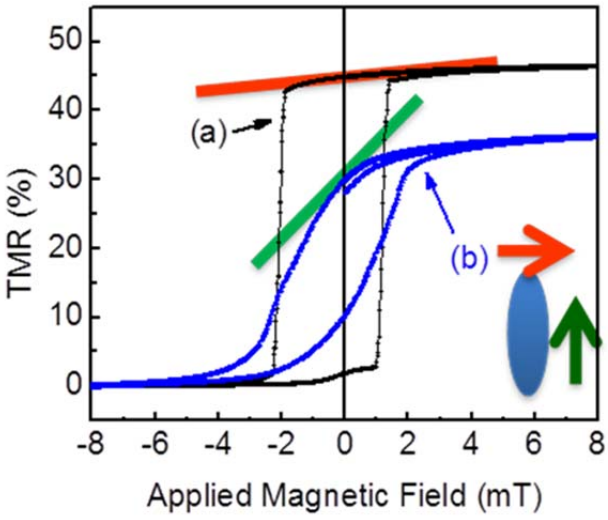

Fig. 6. TMR ratio versus applied magnetic field with different annealing treatments. (a) The loop with dot is the sample that annealed at 300 ^{o}C under 1T magnetic field in the direction along the short axis of the ellipse. (b) TMR loops with triangle dots are the samples that annealed at 300 ^{o}C under 1 T magnetic field along the short axis and, then, annealed at 350 ^{o}C under 0.1 T along the long axis of the ellipse. The slopes of the TMR loops at zero-magnetic field were marked in red and green lines to illustrate the changing sensitivity by the annealing.

Fig. 7 TMR ratio verses applied magnetic field. The samples annealed at 300 ^{o}C under 1 T magnetic field along short axis, and then annealed 350oC under 0.1 T along the long axis of the ellipse. The junctions were patterned into ellipses with a size of 5 μm x 20 μm by photolithography. Tunneling Magnetoreisistive ratio is 250%.

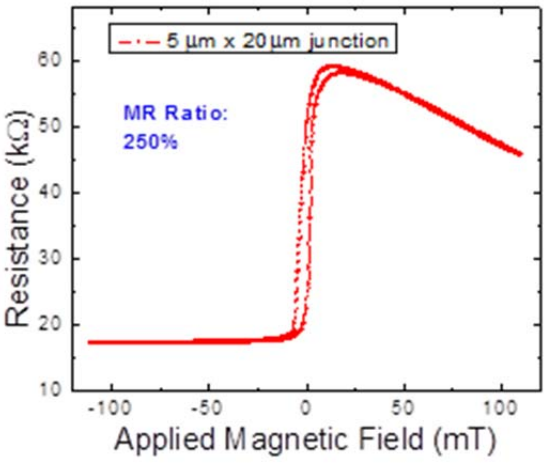

Improving sensitivity of MR sensors using Magnetic Flux Concentrator (MFC)

The magnetic flux concentrator was made using a Conetic alloy which was annealed under hydrogen environment at 1150 ^{o}C for 20 hours with cooling rate about 1 ^{o}C/min. The

sensitivity is increased for a sensor with magnetic flux concentrator. A new design of magnetic flux concentrators (MFC) are shown in Fig 8. The gain of this MFC's is increased from 77 times (without cut a notch) to 134 times (with a notch).

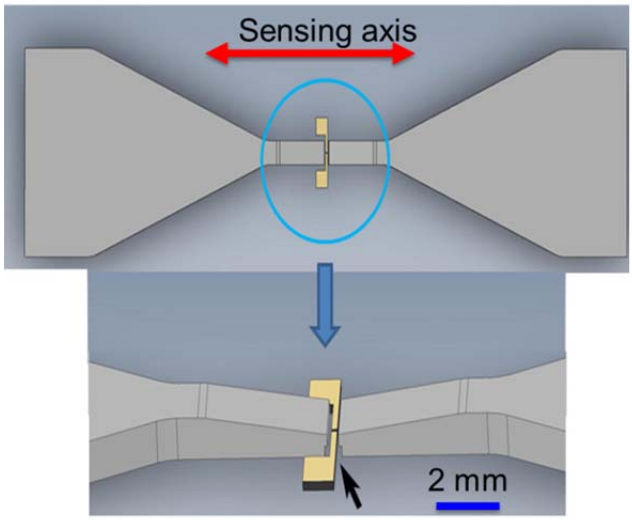

Fig. 8 a New designs of magnetic flux concentrators (MFC) with a gain of 134 times. (The black arrow indicates the position of the notch. The sensing axis is shown by red arrows)

The field in the magnetic sensor bridge enhanced by the magnetic flux concentrator by a factor of 134. In Fig. 9, we show that the sensitivity of this magnetic sensor as high as 4703 %/ mT has been achieved. The magnetic sensor was operated under applied voltage of 1 Volt. Output voltage of the magnetic sensor is linear dependent on the DC magnetic field in the field range of 300 nT. The linear field sensing range is reduced as compared with the junction without the flux concentrator (see Figure 9).

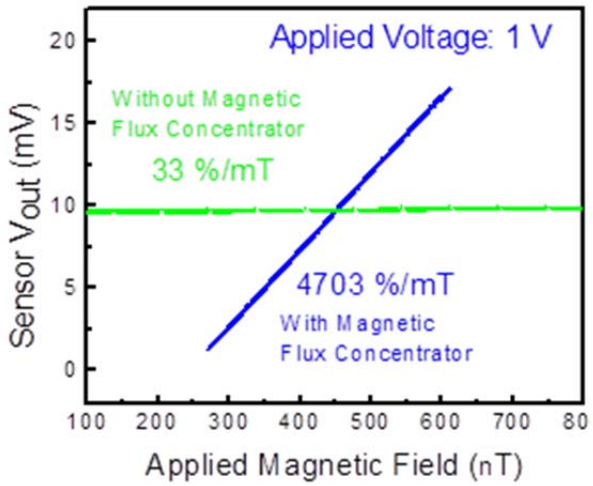

Fig. 9 Output voltage of the magnetic sensor response to DC magnetic field range of 300 nT. The magnetic sensor was operated under the applied voltage of 1 V. The sensitivity of this magnetic sensor is 4703 %/ mT. The signal of an MTJ bridge with magnetic flux concentrators increases by a factor of 134. The definition of the sensitivity is shown in the box.

$$Sensitivity = \frac{V_{out}}{V_{in}} / \Delta B$$

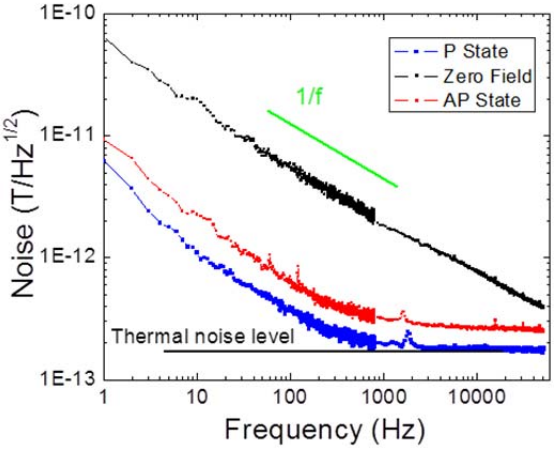

Fig. 10. Noise versus frequency of the MTJ with junction size 30 μm in diameter measured under the applied voltage at 1 V at zero-magnetic fields and the applied magnetic field at -10 mT (AP state) and 10 mT (P state).

We have studied low frequency noise and sensitivity of the MTJ junction. We measured the noise of the MTJ bridge in the frequency range from 1 to 5 x 10^4 Hz with 0 T biasing fields. We have also studied the noise spectrum of the MTJ under the applied magnetic field at 10 mT (parallel state) and the applied magnetic field at -10 mT (antiparallel state), as shown in Fig. 10. It shows that the magnetic noise is about an order magnitude higher in these MTJ sensors. The magnetic field noise was calculated by dividing the voltage noise spectrum measured at the bridge outputs by the bridge sensitivity dV/dB taken from Fig. 9. At an applied voltage of 1 V across the bridge and zero applied magnetic field, the sensitivity is 47030 V/T. The noise level at 1 Hz is 1 μV/$Hz^{1/2}$ giving a field noise of 1 μV/$Hz^{1/2}$/ 47030 V/T = 21 pT/$Hz^{1/2}$. At 1 kHz, the field noise is about 2 pT/ $Hz^{1/2}$. The noise spectrum was fitted with the calculated thermal noise for the measured value of resistance. Hooge-like parameter is about 5 x 10^{-9} μm^2, which is about the same order of magnitude as that reported by Stearrett *et al*.

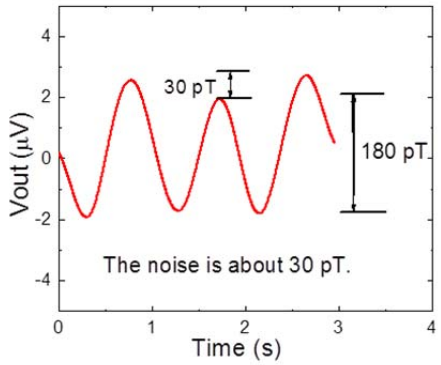

Fig. 11 The magnetic response curve. magnetic sensor output vs. time under a variation of magnetic field at 1 Hz and amplitude of 180 pT.

Fig. 11 shows a real-time magnetic response curve of the magnetic sensor that was measured under an ac variation of magnetic field at 1 Hz and amplitude of 180 pT. The applied voltage on the sensor bridge is at 1 V and under ambient condition. The magnetic sensor was placed inside a coil and the signal was collected with a low-noise amplifier (gain was set at 100) and an A/D convertor. The magnitude of the sensor voltage output is about 2 μV. It is not a perfect sinusoid curve. The distortion may due to the thermal fluctuation of the magnetic domain in the free layer of the magnetic sensor. However, one can see that the peak-to-peak output voltage is much higher than the noise level of about 30 pT.

Task 1b: Design of a low noise amplifier for the MTJ sensor

We have designed a low noise amplifier for the MTJ sensor. The bandwidth of the amplifier is from DC to 50 kHz. The bias supply, gain stage and low pass filter were incorporated into the amplifier. The amplifier will boost the output from the MTJ sensor so the data acquisition (DAQ) can read the response directly, and the low-pass-filter (LPF) is for the anti-anlasing during the data collection. The corner frequency of the LPF is 35 kHz (see Fig. 14).

The sensor amplifier has been tested with MTJ bridges. Each element of the bridge in the range of 5 Kohm to 100 Kohm can be matched. The amplifier contains a bias supply for the bridge (with multiple levels), an instrumentation amplifier (with impedance of 1 Mohm to each input) connected to the bridge, and an anti-aliasing filter after the amplifier. The different gains and different bias voltages were set by a switch. A 1-pole high pass filter (at 3 Hz) to block DC offset can be switched in or out as needed. The system can operate from one 9 V battery inside the electronics enclosure, or optionally, a remote +/-5V supply can be used. During induction measurement, we also added another DC block (1 pole, 5 Hz) to let only the AC component to the preamplifier. The preamplifier needs a gain of 5 to 10 to maintain its low noise performance. For a preamplifier with a gain, it is important to avoid the saturation of the preamplifier by the high DC Earth field – that is the reason to add the DC block. The high-pass-filter (HPF) in the amplifier is redundant.

The MTJ sensor responses both DC and AC magnetic field. It is possible to measure the DC and AC simotaneously: 1) add another Preamplifer before the DC block to measure the DC field directly, no HPF after this preamplifier . Since the input impedance of the preamplifier is high (about Mohm), the additional preamplifier shall not change the performance of the amplifier for the AC measurement. Two DAQ channels are required for this approach. 2) with the existing amplifier but does not use the DC block and the HPF. In that case, it is important to cancel the Earth field by a cancellation coil. The amplifier output is recorded by a single DAQ channel, and software separates the DC and AC components. We will demonstrate the dual-mode detection during the Year 2 effort.

The amplifier response (typical) is shown in Fig. 14. The amplification can be adjusted by the preamplifier gain and the 2nd stage gain. We also characterized the noise of the amplifier, and ensured its voltage noise at the input is few times lower than the voltage noise at the junction output It is important to set the preamplifier gain properly to make sure its input noise is lower than the MTJ voltage noise.

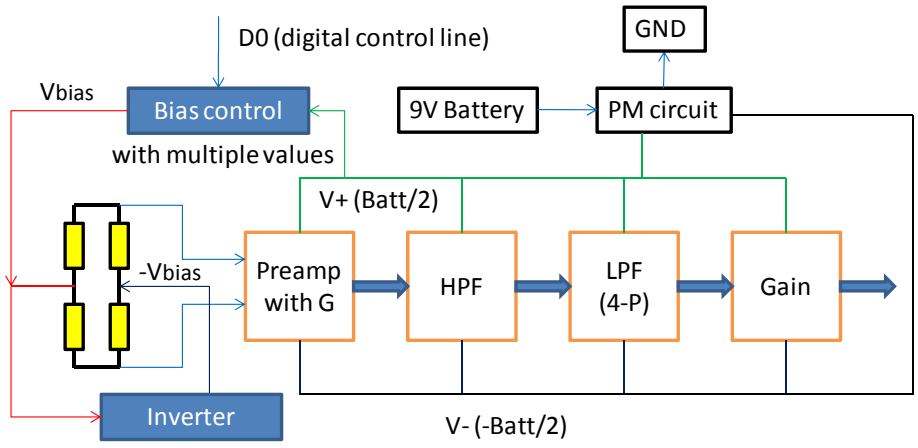

Fig. 12 – Block dirgram for the amplifier

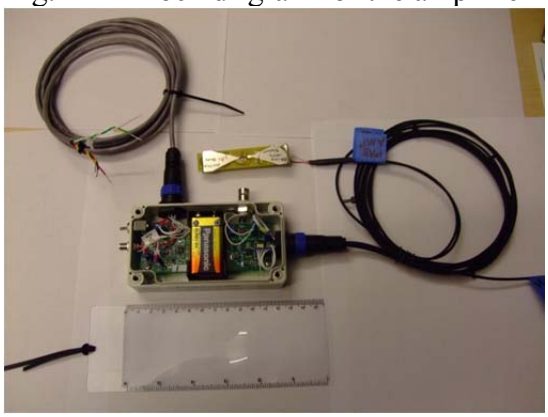

Fig. 13 A low noise amplifier for the MTJ sensor

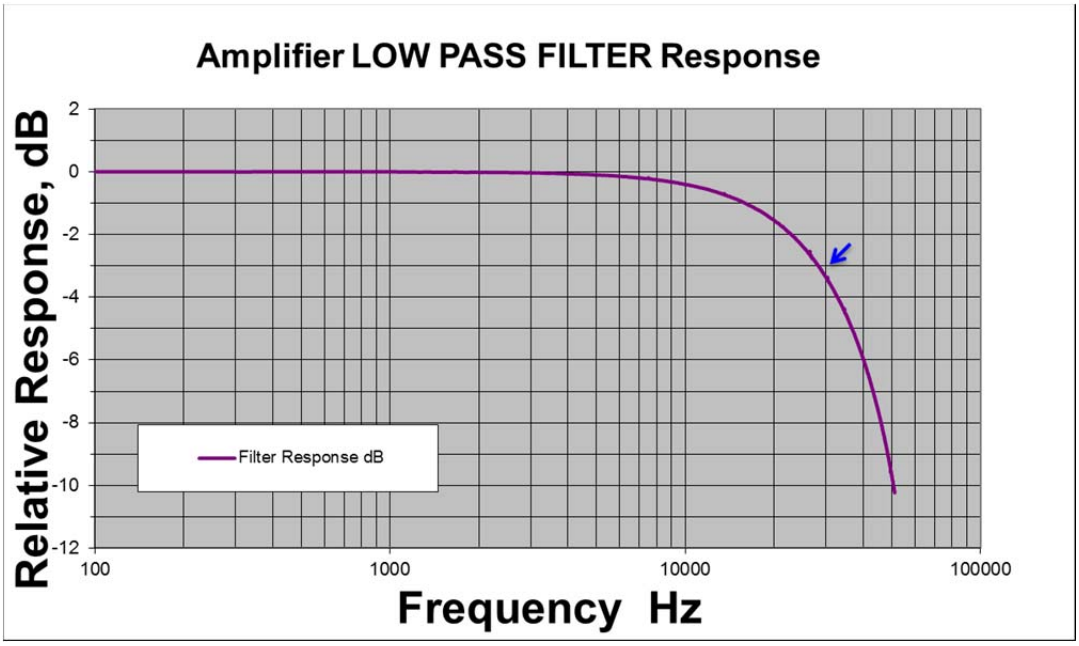

Fig. 14 Response curve of the low noise amplifier for the MTJ sensor. The 3-dB corner for the low-pass filter is at 35 kHz.

Fig. 15 show the sensor response and noise. The amplifier gain G (V/V) was measured first (G = Vout/Vin), and the sensor gain was measured in a calibration coil that is inside the magnetic shield (zero DC field). The sensor output voltage was measured versus the applied B field, and the Sensor Gain (V/T) = Vout/B/G. As we can see from the curves, the sensor gain depends on the bias voltage linearly, and is flat over the band till few kHz. We believe the roll off of the response above few kHz is from the flux concentrator which is made of mu-metal. The sensor noise was measured by placing the sensor in the magnetic shield that has zero magnetic field. The sensitivity of the sensor, as shown in Fig. 15, is the minimum magnetic field the sensor can detect with a signal to noise ratio of 1. It was characterized by measuring the output voltage noise spectrum Vn ($V/Hz^{1/2}$), and by dividing it by the sensor gain at that frequency point, Bn ($pT/ Hz^{1/2}$) = Vn/ Sensor Gain. Both the gain and the output noise follow the roll-off at high frequencies, but their ratios cancel the roll-off.

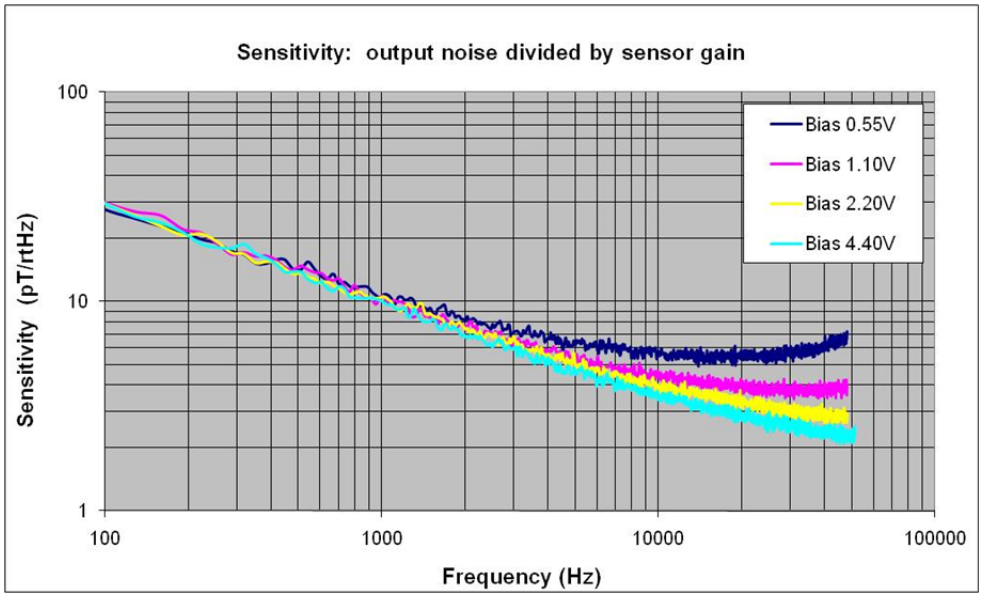

Fig. 15 Sensitivity of MTJ sensor with amplifier designed by QFS, MTJ sensor provided by UNL at the maximum gain of the amplifier (256).

Task 2: Develop of dual-mode sensors

For year 1, we have studied the target response of the MTJ sensor and demonstrated Go/NoGo decision point.

Task 2a: Measurement of standard target response of the MTJ sensor and Go/NoGo decision point

In this task, we will characterize the pulse response of the MTJ sensor in the QFS transmitter coil, using the system (hardware and software) developed for the MM-1444 project. The impulse response of the sensor will be measured and recorded. The results can be feed back to the design of a flux concentrator.

Measurement Setup

Amplifier constructed with adjustable gain, AC/DC coupling, and DC cancellation driver

MTJ Sensor in PVC pipe. Cancellation coils installed on outside. DC to cancel Earth's field, AC to cancel Tx Pulse

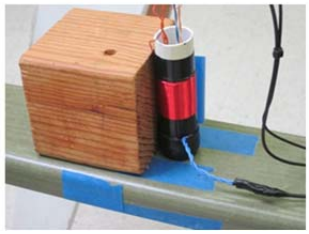

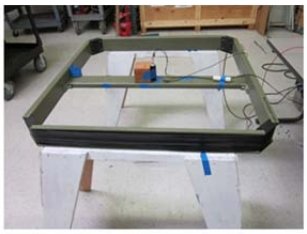

MTJ sensor test bed: 480 Am^2 Tx coil, H-bridge driver, LabVIEW DAQ

Fig. 16 Measurment setup for testing the standard target response of our MTJ sensor
In the practical application for the UXPO detection, the Earth magnetic field is in the order of 0.5 Gauss. With the flux concentrator (with a gain about 100 (see discussion in section D), the DC magnetic field at the MR junction can be as high as 50 Gauss (= 5mT) which could bias the junction at the non sensitive region. A DC field cancellation coil is needed to cancel the DC field along the sensor axis. In the system design, a second MR junction without flux concentrator, aligned to the same direction can be used to provide the reference signal for cancel the DC Earth field, but not the local field, so the sensor stays at the sensitive region (near zero field). We can utilize the bi-polar pulse for the transmitter to remove background noise, with the summation of responses from the top curve (corresponding to falling edge of the positive pulse) and from the bottom curve (corresponding to the rising edge of the negative pulse).

Results for supporting Year 1 GO/NO GO Decision Points:

Prove the feasibility of developing a MgO-based magnetic tunnel junction(sensor); and showing its impulse response to a primary pulse field decaying from a peak field of 0.1 mT to 100 pT within 100 μs measurement of standard target response

In this task, our measurement setup is as follows:
(1) We constructed an amplifier with adjustable gain, AC/DC coupling, and DC cancellation driver.
(2) We place the MTJ Sensor in a small PVC pipe with cancellation coils that installed outside of pipe. The DC cancellation coil is used to cancel the DC Earth field by monitoring the DC output before the DC block, and the AC cancellation coil is used to cancel Tx pulsed field. The AC cancellation coil is taped out from the Tx coil so it has the same time response as the Tx coil, and its number of turns are optimized (with a scope) to minimize the Tx induced sensor response when there is no target. The sensor was placed in the middle of Tx coil inside a PVC pipe against a wood block, aligned vertically.
(3) The MTJ sensor test bed includes a 480 Am^2 Tx coil, H-bridge driver, LabVIEW DAQ etc.
(4) The size of the steel rod target is 2 inches in diameter and 6 inches tall.

MTJ sensor magnetic (DC) response performance:
The DC performance was measured without the DC block before the preamplifier. Also, the gain for the preamplifier was reduced to a lower value. The sensor response shown in Figure 17 was the response without target (background, after the Earth field has been cancelled by the cancellation coil) and with target (at two different distances). In comparison with the fluxgate sensor developed in MM-1444 (which has a r.m.s. input noise of 1-2 nT), the MTJ sensor shows a better stability and low noise (~ 0.3 nT) in the DC operation mode and has a similar target response (~70 nT at 0.55 m, 20 nT at 0.75 m). It also required much lower bias current (few mA) than the fluxgate sensor which requires at least 10X more current for the device.

Both the background and the target response show drift, with a rate about 5nT/20s = 0.25 nT/s during the 1st 20 seconds (for the background), and 15nT/100s = 0.15 nT/s during the 100 sec window (for the background). The drift for the target response during the 20sec measurement window is in the same order, about 0.25 nT/s. This change may due the slow change of the Earth field. It is possible to compensate the drift by monitoring the DC Earth field with a reference sensor, and adjust the current to the cancellation coil based on the reference sensor output.

MTJ sensor induction (AC) response performance:

The target response is characterized at multiple positions beneath the ransmitter/Receiver. The simulated UXO target (steel rod) is stepped through at 1 m x 1 m test grid, with 10 cm spacing. The response is measured at each site in the grid and the target is moved to the next location. Before data collection begins, a background signal is measured (induction response with no target in place), and subtracted from all subsequent data. The location of maximum signal occurs when the target is directly beneath the sensor.

An example of AC response and target signal is shown in Fig. 18. The red curves shows the background signal, present in the sensor after the transmit pulse, but with no target in place. The green trace shows the same measurement, with the target placed 0.5 m directly beneath the coil. The typical visualization of this data is shown in blue. The green trace is subtracted from the red trace, effectively removing the background, and leaving only the target signal. The blue trace is plotted against the right axis. It is evident that a strong and persistent target signal is present from the simulated UXO. The data appears to be well behaved as soon as 10 μs after the transmit pulse. From this Figure it appears that the sensor recovers from the transmit field much faster than the QFS induction sensor; which requires ~ 200 μs for transient recovery.

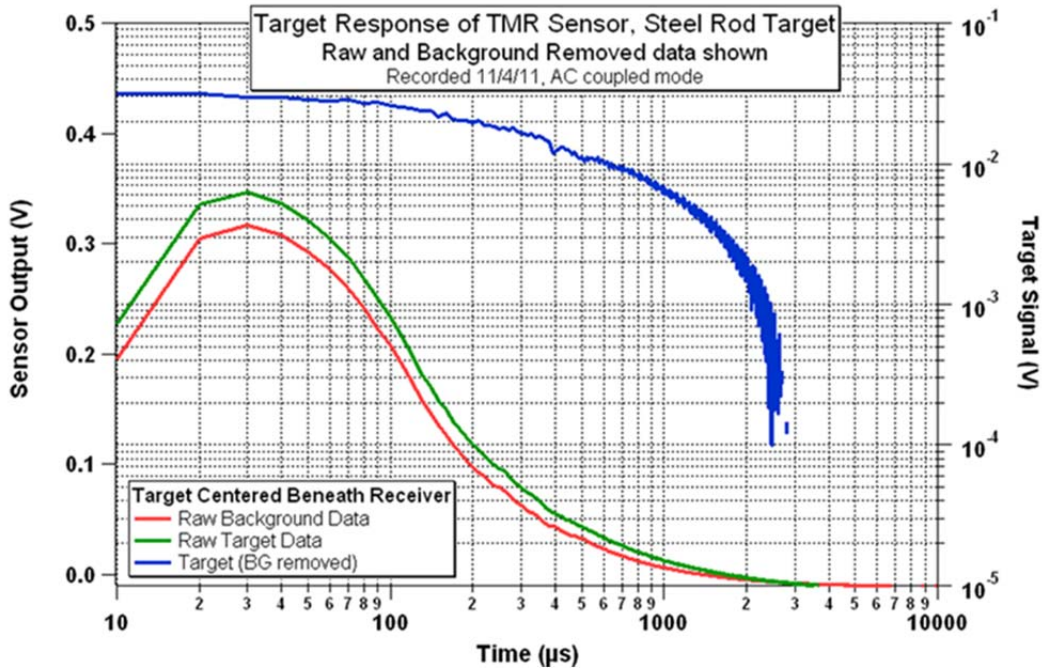

Fig. 18 AC response of our MTJ sensor to 2 inches in diameter and 6 inches tall steel rod. The background curve (red), the target response (green), and difference between the target response and the background (blue) are plotted.

The data collected over the entire test grid can be viewed as a surface plot. The target signal, at a particular time from the 10 μs of decay, is plotted for each location on the grid. The signal from the target can be modeled as a vertical magnetic dipole, and applied over the same test grid as the experiment. A calculated surface plot is shown in Fig. 19 (VMD model plot), for a 0.03 Am^2 vertical magnetic dipole. The function is center peaked, with maximum amplitude directly beneath the receiver.

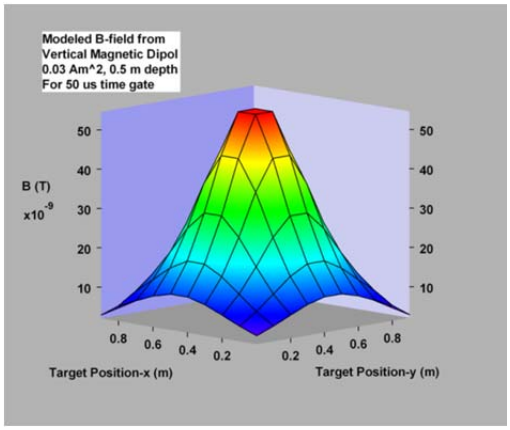

Fig. 19 Modeled B-field form a vertical dipole 0.03 Am^2 at depth of 50 cm, time gate = 50 μs.

AC response of a vertical-aligned MTJ sensor to 50 mm steel rod (2" diameter, 6" tall Steel aligned vertically) over the grid, at depth of 55 cm, time gate = 50 μs following the transmit pulse; a surface plot response is shown in Fig. 20(a) (50 μs surface). The response is center peaked as expected, however the edges of the plot are skewed from 0. This is likely due to imperfections in the background subtraction at the early time after the transmit pulse.

As the primary field transmits field decays, the background becomes more regular and can be subtracted more reliably. A surface plot of target response at 300 μs is shown in Fig. 20 (b). The response is once again center peaked, but now the edges of the grid are also well behaved. For this particular TMR sensor well behaved grid edges were measured around 200 μs (data not shown).

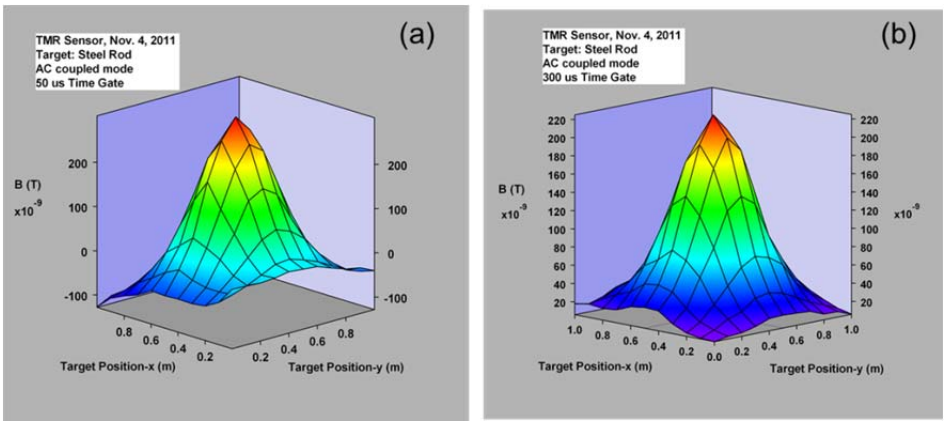

Fig. 20 AC response of a vertical-aligned MTJ sensor to 50 mm steel rod (2" diameter, 6" tall Steel aligned vertically) over the grid, at depth of 55 cm, time gate = 50 μs (a) and 300 μs (b). The sensor is biased at 1.1V, with an amplifier gain of 80. (FOM =0.01 V/nT, Tx =480 Am^2 d=0.55 m, AC coupled)

SUMMARY:

In summary, we demonstrate a simple low-power, magnetic sensor system suitable for high sensitivity magnetic field mapping, based on solid-state magnetic tunnel junction (MTJ) devices with minimum detectable fields in about 30 picotesla range at room temperature. We have proved the feasibility of developing a MgO-based magnetic turnel junction sensor - its impulse response to a primary pulse field decaying from a peak field of 0.1 mT to 100 pT within 100 μs measurement of standard target response. It demonstrates that we have achieved the Year 1 Go/NoGo requirements.

Our MgO based magnetic tunnel junction with a MR ratio as high as 250% has been achieved. This sensor has a sensitivity as high as 4703 %/mT. The magnetic sensor only dissipates 1 mW of power while operating under an applied voltage of 1 V.

It is evident that the TMR sensor measures the expected target response from a simulated UXO object. The sensor shows response as early as 10 μs following the transmit pulse, but with less than perfect SNR on the edges of the test grid. This early time data could be very useful for detection of small objects, provided they are within the inner (high SNR) region of the transmit coil. Through further improvements of the sensor, anti-pulse coil, and possibly transient recovery of the transmitter it may be possible to improve the "edge" SNR of the early time data. At 300 μs the signal matches the model with excellent agreement, SNR is > 200, and the background subtraction is well behaved.

APPENDICES:

Publications:

1. Xiaolu Yin, S. H. Liou, A. O. Adeyeye, S. Jain, and Baoshan Han, "Influence of magnetostatic interactions on the magnetization reversal of patterned magnetic elements", J. Appl. Phys., 109, 07D354 (2011)
2. S. H. Liou, Xiaolu Yin, Stephen E. Russek, Ranko Heindl, F. C. S. Da Silva, John Moreland, David P. Pappas, L Yuan and J. Shen, "Picotesla Magnetic Sensors for Low Frequency Applications", IEEE Trans. on Magnetics, 47, 3740(2011).

Presentations:

1. Xiaolu Yin, S. H. Liou, Adekunle O Adeyeye, Baoshan Han, "Influence of magnetostatic interactions on the magnetization reversal of patterned magnetic elements", Presented at 55th Annual Conference on Magnetism and Magnetic Materials, Atlanta, GA, November 14-18, 2010.
2. Xiaolu Yin, Damien Le Roy, Brady Gilg, Rui Zhang, Ralph Skomski, S. H. Liou, David J. Sellmyer, "Magnetization reversal behaviors of pattered Fe-alloy/Fe:SiO2 multilayers", Presented at 55th Annual Conference on Magnetism and Magnetic Materials, Atlanta, GA, November 14-18, 2010.
3. S. H. Liou, Xiaolu Yin, Stephen E. Russek, Ranko Heindl, F. C. S. Da Silva, John Moreland, David P. Pappas, L Yuan and J. Shen, "Picotesla Magnetic Sensors for Low Frequency Applications", Presented at IEEE International Magnetics Conference, Taipei, Taiwan, April 25-29, 2011.
4. Xiaolu Yin, S. H. Liou, Stephen E. Russek, Ranko Heindl, F. C. S. Da Silva, John Moreland, David P. Pappas, L. Yuan and J. X. Shen "Low Frequency Magnetic Noise in Magnetic Tunnel Junction Arrays", Presented at 2011 Center for Integrated Nanotechnologies user conference, Sep. 14-16, 2011 in Albuquerque, NM.
5. Xiaolu Yin and S. H. Liou, Stephen E. Russek, Ranko Heindl, F. C. S. Da Silva, John Moreland, David P. Pappas, L. Yuan, and J. X. Shen, "Develop Magnetoresistive Sensors for both DC and EMI Magnetic Field Mapping", Partners in Environmental Technology Technical Symposium & Workshop November 29- December 1, 2011, at the Marriott Wardman Park Hotel in Washington, D.C.